Eur. Phys. J. D **42**, 259–267 (2007)
DOI: 10.1140/epjd/e2007-00041-9

THE EUROPEAN
PHYSICAL JOURNAL D

The aluminum arsenides Al_mAs_n $(m + n = 2–5)$ and their anions: Structures, electron affinities and vibrational frequencies

L. Guo[a] and H.-S. Wu

School of Chemistry and Material Chemistry, Shanxi Normal University, Linfen 041004, P.R. China

Received 27 June 2006 / Received in final form 14 September 2006

Abstract. Geometries, electronic states and electron affinities of Al_mAs_n and $Al_mAs_n^-$ $(m + n = 2–5)$ clusters have been examined using four hybrid and pure density functional theory (DFT) methods. Structural optimization and frequency analyses are performed using a 6-311+G(2df) one-particle basis set. The geometries are fully optimized with each DFT method independently. The three types of energy separations reported in this work are the adiabatic electron affinity (EA_{ad}), the vertical electron affinity (EA_{vert}), and the vertical detachment energy (VDE). The calculation results show that the singlet structures have higher symmetry than that of doublet structures. The best functional for predicting molecular structures was found to be BLYP, while other functionals generally underestimated bond lengths. The largest adiabatic electron affinity, vertical electron affinity and vertical detachment energy, obtained at the 6-311+G(2df)/BP86 level of theory, are 2.20, 2.04 and 2.27 eV (AlAs), 2.13, 1.94 and 2.38 eV ($AlAs_2$), 2.44, 2.39 and 2.47 eV (Al_2As), 2.09, 1.80 and 2.53 eV (Al_2As_2), 2.01, 1.57 and 2.36 eV ($AlAs_3$), 2.32, 2.11 and 2.55 eV (Al_2As_3), 2.40, 1.45 and 3.26 eV ($AlAs_4$), 1.94, 1.90 and 2.07 eV (Al_4As), respectively. However, the BHLYP method gives the largest values for EA_{ad} and EA_{vert} of Al_3As and EA_{ad} of Al_3As_2, respectively. For the vibrational frequencies of the Al_nAs_m series, the B3LYP method produces good predictions with the average error only about 10 cm^{-1} from available experimental and theoretical values. The other three functionals overestimate or underestimate the vibrational frequencies, with the worst predictions given by the BHLYP method.

PACS. 31.15.Ew Density-functional theory – 36.40.-c Atomic and molecular clusters

1 Introduction

The III-V semiconductor clusters have been the topic of many experimental and theoretical studies [1–3]. A primary driving force behind such studies is that III-V materials are of great technological importance, since they have applications in the fabrication of fast microelectronic devices, small devices, and light-emitting diodes. Consequently, a detailed study of the properties of such clusters as a function of their size could provide significant insight into the evolution from the molecular level to the bulk. Despite the numerous experimental investigations of GaAs, InAs, InP, and more recently, AlP and GaP clusters, the literature contains very little on the AlAs clusters. Ab initio calculations on properties of Al_xAs_y clusters have been carried out by several groups [4–10]. Andreoni [4] calculated the structures, stability, and melting of $(AlAs)_n$ $(n = 2–5)$ using the Car-Parrinello method. Quek et al. [5] reported tight binding molecular dynamics studies of the structures of Al_mAs_n $(m + n \leqslant 13)$. Tozzini et al. [6] presented extensive theoretical calculations of the geometric and electronic properties of neutral and ionized AlAs fullerene-like clusters of the type Al_xAs_{x+4} with a number of atoms up to 52, on the basis of density functional theory. Costales et al. [7] used density functional theory (DFT) to explore structural and vibrational properties for $(AlAs)_n$ clusters up to 6 atoms, finding the same behavior as in the Aluminum nitride clusters. Archibong et al. [8] calculated the low-lying electronic states of Al_3As, $AlAs_3$, and the corresponding anions at the B3LYP and CCSD(T) levels of theory using the 6-311+G(2df) one-particle basis set. The adiabatic electron affinities, electron detachment energies and harmonic vibrational frequencies of both the anions and the neutral molecules are presented and discussed. Feng et al. [9] reported a MRSDCI study of the ground and several low-lying excited states of Al_2As_3, Al_3As_2, and their ions. Recently, Zhu [10] studied the spectroscopic properties for Al_2As, $AlAs_2$, and their ions using density functional theory (DFT:B3LYP) and complete active space multiconfiguration self-consistent field (CASSCF) calculations. The theoretical prediction of Al_xAs_y electron detachment energy and electron affinities is found in the 2002 study of Archibong et al. [8]. To our knowledge, this is the first time anyone has studied the geometries and electronic affinities of Al_4As and $AlAs_4$ using density functional theory.

---

[a] e-mail: `gl-guoling@163.com`

Density functional theory (DFT) [11,12] has evolved into a widely applicable computational technique, while requiring less computational effort than convergent quantum mechanical methods such as coupled cluster theory. The application of gradient-corrected density functionals theory has been shown to be effective for many species in groups III and V such as Ga_xP_y ($x = 1$; $y = 1, 2$), Al_xN_y ($x = 1$–6, 12, 13; $y = 1$), and In_xN_y ($x = 1$–2; $y = 1$–2) [13–15]. The theoretical prediction of electron affinities has historically been generally difficult. The main reasons are the significance of electron correlation and the special requirements of the anionic systems with regard to the one-electron basis sets. Hence, in the traditional ab initio systems one needs highly correlated methods and large and flexible (in particular in the outer area which requires additional diffuse functions) basis sets. While for DFT employing local functionals there are principal difficulties with anions, from a pragmatic point of view these deficiencies are not severe; and recent work [8] has shown that the DFT methods are dependable for EA predictions.

The objective of the present study is to systematically apply several contemporary forms of density functional theory [11] to the determination of the electron affinities and other properties of the Al_mAs_n ($m + n = 2$–5) series. Of specific interest is (a) the comparison of the electron affinities with the limited available calculational results; (b) the relationship between the neutral Al_mAs_n molecules and their anions as measured by the three types of energy separations, e.g., the adiabatic electron affinity (EA_{ad}), the vertical electron affinity (EA_{vert}), and the vertical detachment energy of the anion (VDE); (c) the prediction of vibrational frequencies; and (d) comparison of the different DFT methods. We would like to establish reliable theoretical predictions for those aluminum arsenides in the absence of experimental results and in some cases to challenge existing experiments.

2 Theoretical methods

The four different density functional or hybrid Hartree-Fock/ density functional forms used here were as follow:

(a) Becke's 1988 exchange functional with Lee, Yang and Parr's correlation functional [16] (BLYP);
(b) the half and half exchange functional [17] with the LYP correlation functional (BHLYP);
(c) Becke's three-parameter hybrid exchange functional [18] with the LYP correlation functional (B3LYP) [18]; and
(d) Becke's 1988 exchange functional with Perdew's correlation functional [19] (BP86).

Restricted methods were used for all closed-shell systems, while unrestricted methods were employed for the open-shell species. All the electron affinities and molecular structures have been determined using the Gaussian 98 [20] program suites.

The basis set employed in this study was the 6-311+G(2df) one-particle basis set [26,27], which was similar to that employed by Achibong and St-Amant in their previous work on small clusters of germanium [21], aluminum oxides [22–24] and GaP^-/GaP_2^- [25].

All Al_mAs_n ($m + n = 2$–5) stationary point geometries are interrogated by the evaluation of their harmonic vibrational frequencies at the four different levels of theory. Zero-point vibrational energies (ZPVE) evaluated at the four levels are presented in Table 3. The ZPVE differences between Al_mAs_n and $Al_mAs_n^-$ ($m+n = 2$–5) are quite small. These differences could be used as a correction to the adiabatic electron affinities.

The electron affinities are evaluated as the difference of total energies in the following manner: the adiabatic electron affinity is determined as

$$EA_{ad} = E\ (\text{optimized neutral}) - E\ (\text{optimized anion})$$

the vertical electron affinity by

$$EA_{vert} = E\ (\text{optimized neutral}) - E\ (\text{anion at optimized neutral geometry})$$

and the vertical detachment energy of the anion by

$$VDE = E\ (\text{neutral at optimized anion geometry}) - E\ (\text{optimized anion}).$$

3 Results and discussion

The ground state structures of Al_mAs_n and $Al_mAs_n^-$ ($m+n = 2$–5) optimized by four hybrid and pure density functional theory (DFT) methods are shown in Figure 1. The corresponding geometric parameters of Al_mAs_n and $Al_mAs_n^-$ are listed in Tables 1 and 2, respectively.

3.1 m + n = 2

AlAs and AlAs⁻

The geometries of the ground state of AlAs and its anion are given in 1n and 1a in Figure 1. The neutral AlAs has a X $^3\Sigma^-$ ground state. Costales and Kandalam [7] reported a theoretical bond length of 2.570 Å at the GGA level of theory in conjunction with a double numerical basis set supplemented with *d* polarization functions. The present 6-311+G(2df) BLYP bond length (2.341 Å) provides the most favorable comparison with the previous theory, while the other DFT methods predict shorter bond lengths by up to 0.28 Å (BHLYP). The general trend for bond lengths for the aluminum arsenide is BLYP > BP86 = B3LYP > BHLYP.

For the $^2\Pi$ ground state of the diatomic anion $AlAs^-$, the predicted bond agree with each other to 0.1 Å among the different DFT methods, with the r_e values being roughly 0.1 Å shorter than those of the neutral species. The 6-311+G(2df) BLYP bond length, deemed to be the most reliable, is 2.258 Å.

Our theoretical neutral-anion energy separations for AlAs are given in Table 4. No experimental or other theoretical data is available. The adiabatic electron affinity EA_{ad} is predicted to be 1.90 eV (BHLYP), 2.03 eV

Table 1. Geometric parameters and symmetry of neutral Al_mAs_n ($m+n=2$–5).

Structure	State	Symmetry	BHLYP		B3LYP		BP86		BLYP	
			Type	L/Å (A/°)	Type	L/Å (A/°)	Type	L/Å (A/°)	Type	L/Å (A/°)
AlAs (1n)	$^3\Sigma$	$C_{\infty v}$	1–2	2.313	1–2	2.323	1–2	2.323	1–2	2.341
$AlAs_2$ (2n)	$^2B_2$	C_{2v}	1–2	2.711	1–2	2.741	1–2	2.739	1–2	2.777
			2–3	2.167	2–3	2.194	2–3	2.208	2–3	2.225
			2–1–3	47.2	2–1–3	47.2	2–1–3	47.6	2–1–3	47.2
Al_2As (3n)	$^2B_2$	C_{2v}	1–3	2.337	1–3	2.345	1–3	2.345	1–3	2.359
			1–3–2	89.2	1–3–2	92.0	1–3–2	90.5	1–3–2	97.9
Al_2As_2 (4n)	^1A_g	D_{2h}	1–2	2.628	1–2	2.652	1–2	2.653	1–2	2.682
			2–3	2.272	2–3	2.299	2–3	2.309	2–3	2.330
			2–1–3	51.2	2–1–3	51.4	2–1–3	51.6	2–1–3	51.5
$AlAs_3$ (5n)	$^1A_1$	C_{2v}	1–2	2.345	1–2	2.372	1–2	2.383	1–2	2.400
			1–4	2.570	1–4	2.591	1–4	2.584	1–4	2.618
			2–4	2.328	2–4	2.357	2–4	2.367	2–4	2.392
			2–1–3	112.6	2–1–3	113.0	2–1–3	113.5	2–1–3	113.5
			2–4–3	113.9	2–4–3	114.1	2–4–3	114.7	2–4–3	114.1
Al_3As (6n)	$^1A_1$	C_{2v}	1–2	2.646	1–2	2.629	1–2	2.605	1–2	2.638
			2–3	2.351	2–3	2.371	2–3	2.383	2–3	2.397
			2–3–4	115.8	2–3–4	112.5	2–3–4	111.0	2–3–4	110.7
Al_2As_3 (7n)	$^2A''_2$	D_{3h}	1–2	2.543	1–2	2.564	1–2	2.565	1–2	2.591
			2–3	2.514	2–3	2.546	2–3	2.547	2–3	2.581
Al_3As_2 (8n)	$^2A'$	C_s	1–4	2.512	1–4	2.522	1–4	2.518	1–4	2.550
			3–5	2.511	3–5	2.460	3–5	2.463	3–5	2.473
			4–5	2.367	4–5	2.388	4–5	2.395	4–5	2.416
$AlAs_4$ (9n)	$^2A_1$	C_{2v}	1–2	2.453	1–2	2.486	1–2	2.491	1–2	2.523
			2–3	2.476	2–3	2.508	2–3	2.514	2–3	2.543
			3–5	2.389	3–5	2.421	3–5	2.423	3–5	2.453
Al_4As (10n)	$^2A_1$	C_{2v}	1–2	2.499	1–2	2.521	1–2	2.535	1–2	2.549
			1–3	2.554	1–3	2.576	1–3	2.578	1–3	2.606
			2–3	2.823	2–3	2.806	2–3	2.756	2–3	2.814
			3–5	2.607	3–5	2.610	3–5	2.598	3–5	2.628

Table 2. Geometric parameters and symmetry of anionic Al_mAs_n ($m+n=2$–5).

Structure	State	Symmetry	BHLYP		B3LYP		BP86		BLYP	
			Type	L/Å (A/°)	Type	L/Å (A/°)	Type	L/Å (A/°)	Type	L/Å (A/°)
$AlAs^-$ (1a)	$^2\Pi$	$C_{\infty v}$	1–2	2.339	1–2	2.236	1–2	2.242	1–2	2.258
$AlAs_2^-$ (2a)	$^1A_1$	C_{2v}	1–2	2.523	1–2	2.552	1–2	2.561	1–2	2.585
			2–3	2.262	2–3	2.291	2–3	2.302	2–3	2.324
			2–1–3	53.2	2–1–3	53.4	2–1–3	53.4	2–1–3	53.4
Al_2As^- (3a)	$^1A_1$	C_{2v}	1–3	2.334	1–3	2.353	1–3	2.360	1–3	2.375
			1–3–2	102.7	1–3–2	106.7	1–3–2	107.8	1–3–2	111.6
$Al_2As_2^-$ (4a)	$^2B_1$	C_{2v}	1–2	2.533	1–2	2.557	1–2	2.560	1–2	2.586
			2–3	2.429	2–3	2.457	2–3	2.459	2–3	2.489
			1–2–4	117	1–2–4	115	1–2–4	114	1–2–4	115
$AlAs_3^-$ (5a)	$^2A'$	C_s	1–2	2.379	1–2	2.405	1–2	2.410	1–2	2.439
			2–3	2.559	2–3	2.578	2–3	2.575	2–3	2.603
			2–4	2.523	2–4	2.564	2–4	2.573	2–4	2.606
			2–1–3	59.1	2–1–3	59.6	2–1–3	60.0	2–1–3	60.1
			2–4–3	60.5	2–4–3	64.4	2–4–3	64.5	2–4–3	64.6
Al_3As^- (6a)	$^2B_2$	C_{2v}	1–2	2.711	1–2	2.695	1–2	2.666	1–2	2.706
			1–3	2.596	1–3	2.645	1–3	2.667	1–3	2.696
			2–3	2.427	2–3	2.447	2–3	2.457	2–3	2.472
			2–1–4	108.8	2–1–4	109.0	2–1–4	109.7	2–1–4	108.9
$Al_2As_3^-$ (7a)	$^1A'_1$	D_{3h}	1–2	2.642	1–2	2.669	1–2	2.670	1–2	2.703
			2–3	2.458	2–3	2.484	2–3	2.485	2–3	2.516
$Al_3As_2^-$ (8a)	$^1A'_1$	D_{3h}	1–2	2.556	1–2	2.574	1–2	2.568	1–2	2.599
			1–5	2.563	1–5	2.594	1–5	2.603	1–5	2.629
$AlAs_4^{--}$ (9a)	$^1A_1$	C_{4v}	1–2	2.366	1–2	2.401	1–2	2.411	1–2	2.439
			1–5	2.796	1–5	2.822	1–5	2.811	1–5	2.858
Al_4As^- (10a)	$^1A_1$	C_{2v}	1–2	2.535	1–2	2.563	1–2	2.579	1–2	2.596
			1–3	2.497	1–3	2.518	1–3	2.524	1–3	2.546
			2–3	2.791	2–3	2.805	2–3	2.786	2–3	2.829
			3–5	2.605	3–5	2.638	3–5	2.645	3–5	2.673

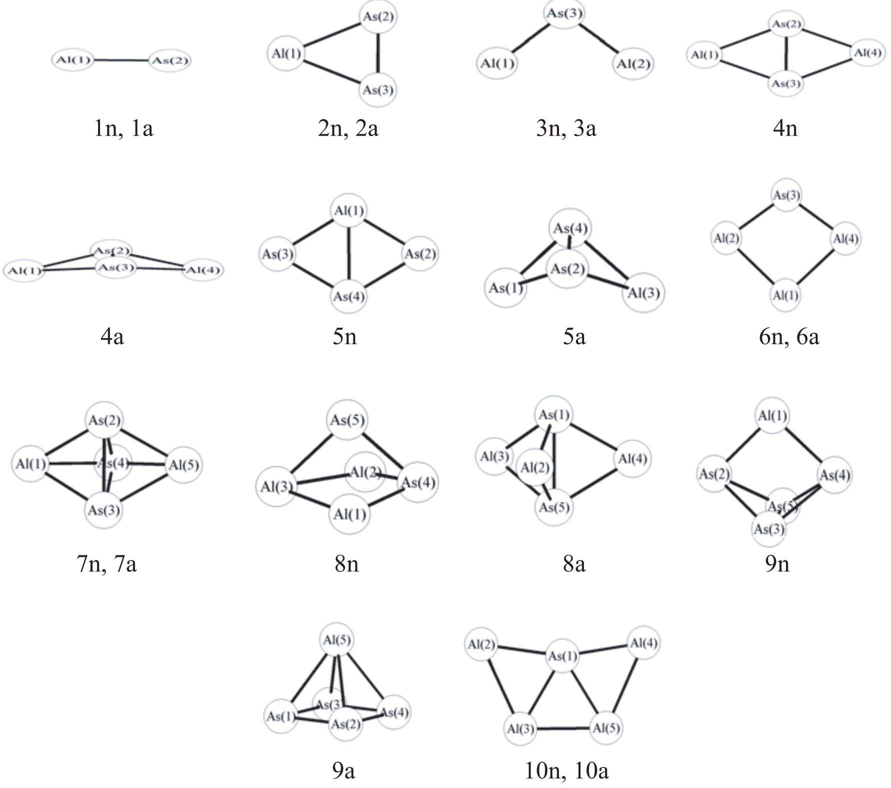

1n, 1a 2n, 2a 3n, 3a 4n

4a 5n 5a 6n, 6a

7n, 7a 8n 8a 9n

9a 10n, 10a

Fig. 1. Geometric configurations of the Al_mAs_n and $Al_mAs_n^-$ ($m + n = 2$–5) clusters (n neutral and a anion).

(B3LYP), 2.20 eV (BP86), and 1.94 eV (BLYP). The zero-point vibrational energy correction is very small, around +0.01 eV (Tab. 3). The range for the theoretical vertical electron affinity EA_{vert} is from 1.80 to 2.04 eV, and the range of VDE ($AlAs^-$) is 1.90–2.27 eV. The general trend for EA_{ad}, EA_{vert}, and VDE for aluminum arsenide is BP86 > B3LYP > BLYP > BHLYP. The values of them are close to each other due to the small difference in geometry between the neutral species and its anion.

3.2 m + n = 3

$AlAs_2$ and $AlAs_2^-$

The equilibrium geometries of the $^2B_2$ ground state of neutral $AlAs_2$ and the $^1A_1$ ground state of $AlAs_2^-$ are displayed in 2n and 2a in Figure 1. For the C_{2v} $AlAs_2$ structure, the theoretical Al-As and As-As bond lengths are in the ranges of 2.711–2.777 Å and 2.167–2.225 Å, respectively. As was case for AlAs, the BLYP method gives the longest and most reliable bond lengths. As-Al-As bond angles of 47.2–47.6° are predicted by four different functions. No experimental geometries are available for either $AlAs_2$ or $AlAs_2^-$. Zhu [10] reported a theoretical bond lengths of 2.706 and 2.226 Å for Al-As and As-As bonds and a bond angle of 48.6° at the CASSCF level of theory. Our BLYP results are the closest to the earlier CASSCF result.

The anion $AlAs_2^-$ also has C_{2v} symmetry, with the Al-As and As-As bond distances predicted to be

Table 3. Zero-point vibrational energies within the harmonic approximation for $Al_mAs_n/Al_mAs_n^-$ ($m + n = 2$–5) in eV (kcal/mol in parentheses)[a].

Molecular	BHLYP	B3LYP	BP86	BLYP
AlAs	0.023(0.53)	0.023(0.53)	0.023(0.53)	0.022(0.51)
$AlAs^-$	0.024(0.56)	0.026(0.61)	0.026(0.61)	0.025(0.58)
$AlAs_2$	0.048(1.11)	0.045(1.04)	0.044(1.02)	0.042(0.97)
$AlAs_2^-$	0.055(1.27)	0.052(1.19)	0.051(1.19)	0.049(1.13)
Al_2As	0.026 (0.60)	0.032(0.74)	0.037(0.84)	0.037(0.84)
Al_2As^-	0.052(1.19)	0.049(1.13)	0.048(1.11)	0.047(1.07)
Al_2As_2	0.080(1.85)	0.077(1.78)	0.077(1.78)	0.073(1.69)
$Al_2As_2^-$	0.080(1.85)	0.077(1.78)	0.078(1.79)	0.072(1.68)
$AlAs_3$	0.099(2.30)	0.095(2.18)	0.093(2.15)	0.089(2.06)
$AlAs_3^-$	0.084(1.94)	0.081(1.86)	0.082(1.88)	0.076(1.76)
Al_3As	0.088(2.04)	0.088(2.04)	0.091(2.09)	0.086(1.99)
Al_3As^-	0.082(1.88)	0.080(1.85)	0.083(1.90)	0.077(1.78)
Al_2As_3	0.130(3.01)	0.127(2.93)	0.129(2.98)	0.122(2.81)
$Al_2As_3^-$	0.123(2.83)	0.117(2.71)	0.119(2.74)	0.111(2.56)
Al_3As_2	0.096(2.22)	0.100(2.31)	0.105(2.43)	0.100(2.31)
$Al_3As_2^-$	0.116(2.67)	0.112(2.58)	0.114(2.63)	0.107(2.47)
$AlAs_4$	0.129(2.98)	0.120(2.77)	0.118(2.71)	0.112(2.59)
$AlAs_4^-$	0.123(2.85)	0.116(2.67)	0.115(2.66)	0.108(2.49)
Al_4As	0.102(2.35)	0.100(2.31)	0.103(2.37)	0.096(2.21)
Al_4As^-	0.113(2.60)	0.107(2.46)	0.105(2.42)	0.099(2.30)

[a] All results obtained with the 6-311+G(2df) basis set.

Table 4. Adiabatic and vertical electron affinities of the neutral Al_mAs_n ($m + n = 2$–5) and vertical detachment energies of their anions in eV (kcal /mol in parentheses)[a].

Molecular	Method	EA_{ad}	EA_{vert}	VDE
AlAs	BHLYP	1.90(44.09)	1.83(42.27)	1.90(44.09)
	B3LYP	2.03(46.92)	1.99(46.23)	2.11(48.68)
	BP86	2.20(50.44)	2.04(47.09)	2.27(52.32)
	BLYP	1.94(44.78)	1.80(41.54)	2.01(46.35)
$AlAs_2$	BHLYP	1.94(44.78)	1.70(39.19)	2.19(50.44)
	B3LYP	2.03(46.92)	1.82(41.90)	2.26(52.04)
	BP86	2.13(49.25)	1.94(44.78)	2.38(54.90)
	BLYP	1.83(42.27)	1.64(37.75)	2.04(47.09)
Al_2As	BHLYP	2.33(53.86)	2.29(52.82)	2.36(54.46)
	B3LYP	2.40(55.40)	2.36(54.58)	2.42(55.96)
	BP86	2.44(56.22)	2.39(55.27)	2.47(56.99)
	BLYP	2.20((50.44))	2.17(50.06)	2.23(51.57)
Al_2As_2	BHLYP	1.95(44.91)	1.62(37.31)	2.40(55.40)
	B3LYP	1.98(45.50)	1.68(38.88)	2.42(55.96)
	BP86	2.09(48.18)	1.80(41.78)	2.53(58.50)
	BLYP	1.75(40.62)	1.46(33.60)	2.21(51.09)
$AlAs_3$	BHLYP	1.99(46.23)	1.52(35.05)	2.35(54.16)
	B3LYP	1.95(44.91)	1.53(35.24)	2.27(52.34)
	BP86	2.01(46.35)	1.57(36.16)	2.36(54.46)
	BLYP	1.69(38.97)	1.46(33.60)	1.98(45.67)
Al_3As	BHLYP	1.88(43.40)	1.57(36.16)	2.04(47.09)
	B3LYP	1.80(41.78)	1.48(34.09)	2.02(46.78)
	BP86	1.84(42.58)	1.52(35.01)	2.09(48.18)
	BLYP	1.52(35.05)	1.20(27.64)	1.77(40.86)
Al_2As_3	BHLYP	2.28(52.65)	2.07(47.76)	2.50(57.54)
	B3LYP	2.32(53.43)	2.10(48.41)	2.55(58.62)
	BP86	2.32(53.43)	2.11(48.68)	2.55(58.62)
	BLYP	2.11(48.68)	1.88(43.40)	2.34(53.73)
Al_3As_2	BHLYP	2.98(68.74)	2.35(54.16)	2.84(65.21)
	B3LYP	2.90(66.85)	2.46(56.70)	2.87(65.90)
	BP86	2.79(64.31)	2.58(59.49)	2.99(68.66)
	BLYP	2.60(59.96)	2.27(52.34)	2.72(62.46)
$AlAs_4$	BHLYP	2.16(49.66)	1.31(30.16)	3.15(73.14)
	B3LYP	2.32(53.43)	1.44(33.10)	3.24(75.20)
	BP86	2.40(55.40)	1.45(33.33)	3.26(75.66)
	BLYP	2.18(50.31)	1.28(29.52)	3.06(71.05)
Al_4As	BHLYP	1.72(39.63)	1.69(39.07)	1.75(40.62)
	B3LYP	1.83(42.27)	1.80(41.78)	1.86(43.17)
	BP86	1.94(44.78)	1.90(44.09)	2.07(48.04)
	BLYP	1.65(38.04)	1.61(37.36)	1.68(38.88)

[a] Values are not corrected for ZPVE and were obtained with the 6-311+G(2df) basis set.

2.523–2.585 Å and 2.262–2.324 Å, respectively. The Al-As bond distances are about 0.2 Å shorter than their neutral counterparts, while the As-As bond distances are about 0.1 Å longer and the bond angles are about 5° larger.

The theoretical EA_{ad} EA_{vert}, and VDE are listed in Table 4. The general trend for the four different functionals is BP86 > B3LYP > BHLYP > BLYP. The range of EA_{ad} is from 1.83 to 2.13 eV for the four different functionals. The range of EA_{vert} is from 1.64 to 1.94 eV and the range of VDE is from 2.04 to 2.38 eV. The values for EA_{ad}, EA_{vert}, and VDE are fairly similar due to the small differences in geometry between the neutral species and its anion.

Al_2As and Al_2As^-

The geometries of the $^2B_2$ ground state of Al_2As and its $^1A_1$ ground state anion are given in 3n and 3a in Figure 1. For the C_{2v} Al_2As structure, the theoretical Al-As bond lengths are in the range 2.337 to 2.359 Å and Al-As-Al bond angles of 89.2–97.9 are predicted by the four different functionals. A theoretical bond length of 2.390 Å was also given by Zhu [10] using the CASSCF level of theory. Our BLYP results are the closet to the earlier result. The other DFT methods predict shorter bond distances.

With attachment of an extra electron to the neutral Al_2As to form the Al_2As^- anion, the symmetry does not change, but the Al-As-Al bond angle changes by 13–18°, and the Al-As bond lengths are longer than those of the neutral by 0.02 Å.

Our theoretical neutral-anion energy separations for Al_2As are given in Table 4. The adiabatic electron affinity EA_{ad} is predicted to be 2.33 eV (BHLYP), 2.40 eV (B3LYP), 2.44 eV (BP86), and 2.20 eV (BLYP). The range for the theoretical vertical electron affinity EA_{vert} is from 2.17 to 2.39 eV, among which the BP86 method again predicts the largest value (2.39 eV). The range of VDE (Al_2As^-) is 2.23–2.47 eV, and thus the anion is quite stable with respect to electron detachment. The BP86 method again predicts the largest value. The values of EA_{ad}, EA_{vert}, and VDE are close to each other due to the small geometry difference between the neutral species and its anion.

3.3 m + n = 4

Al_2As_2 and $Al_2As_2^-$

The equilibrium structures of the ^1A_g ground state of neutral Al_2As_2 and the $^2B_1$ ground of $Al_2As_2^-$ are shown in 4n and 4a in Figure 1. For the D_{2h} Al_2As_2 structure, the theoretical Al-As and As-As bond lengths are in the range 2.628–2.682 Å and 2.272–2.330 Å, respectively, and As-Al-As bond angles of 51.2–51.6° are predicted by the four different functionals. Costales et al. [7] reported a theoretical Al-As and As-As bond lengths of 2.670 and 2.340 Å and a bond angle of 52° at the GGA/DNP level of theory. Our BLYP results are the closest to the earlier GGA/DNP results. The other three DFT methods predict shorter bond distances.

The anionic $Al_2As_2^-$ is found to have no planar C_{2v} distorted tetrahedron ground state (‘butterfly’ structure). Adding an electron makes the Al-As bond distances about 0.1 Å shorter than their neutral counterparts, while the As-As bond distances are about 0.2 Å longer.

The theoretical EA_{ad}, EA_{vert}, and VDE are listed in Table 4. The range of EA_{ad} is from 1.75 to 2.09 eV from the four different functionals. The BP86 method predicts the largest EA_{ad} for Al_2As_2 (2.09 eV). The range of EA_{vert} is from 1.46 to 1.80 eV and the range of VDE is from 2.21 to 2.553 eV. The BHLYP result for VDE (2.21 eV) is again the smallest value. The other three DFT methods predict larger values. The differences between EA_{ad},

EA_{vert}, and VDE are due to the change in the geometry between Al_2As_2 and $Al_2As_2^-$.

$AlAs_3$ and $AlAs_3^-$

The geometries of the ground state of $AlAs_3$ and its anion are displayed in 5n and 5a in Figure 1. The neutral $AlAs_3$ molecule has C_{2v} symmetry for the $^1A_1$ ground state. Archibong and St-Amant [8] have studied the lowlying electronic states of $AlAs_3$ and its corresponding anion at the B3LYP, MP2 and CCSD(T) levels using the 6-311+G(2df) one-particle basis set. They found two singlet states ($^1A_1$-C_{2v} and $^1A'$-C_s) were nearly degenerate. We also optimize these structures and predicte the C_{2v} structure to be the ground state of $AlAs_3$. Archibong and St-Amant reported the two Al-As, As-As bond distances and As-Al-As, As-As-As band angles to be 2.400, 2.331, 2.570 Å and 111.6, 116.8°; 2.372, 2.357, 2.591 Å and 113.0, 114.1°, at the MP2 and B3LYP levels of theory, respectively. Our BLYP results are close to Archibong's results. The other three DFT functionals predict shorter bonds. The bond angles from the different theoretical methods change only slightly.

The $^2A'$ ground state of the $AlAs_3^-$ anion is predicted to have a three-dimensional distorted tetrahedron structure with C_s-symmetry [5a in Fig. 1]. The trend for the theoretical bond lengths with the different theoretical methods is similar to that for the neutral cluster, i.e., BLYP > BP86 > B3LYP > BHLYP. The DFT As-Al-As and As-As-As bond angles range from 59.1 to 60.1° and from 60.5 to 64.6°, respectively. The BLYP method predicts the geometrical parameters to be r(As1-As2) = 2.439 Å, r(As2-Al3) = 2.603 Å, r(As2-As4) = 2.606 Å, and As-Al-As = 60.1°, As-As-As = 64.6°, which are close to Archibong's results of 2.376 Å, 2.606 Å, 2.566 Å, 59.0°, and 65.4° at the MP2 level of theory, respectively. We also tried to optimize structures for the $C_{\infty v}$, C_{2v}, C_{3v} and other C_s symmetry reported by Archibong for $AlAs_3^-$ [8], but these stationary points all have higher energies and some have one imaginary vibrational frequency indicating instability.

The theoretical EA_{ad}, EA_{vert}, and VDE are listed in Table 4. The predicted EA_{ad} for $AlAs_3$ ranges from 1.69 to 2.01 eV. Among them the BP86 method predicts the largest value (2.01 eV) The EA_{vert} values vary from 1.46 to 1.57 eV, while the VDE values are large and vary from 1.98 to 2.36 eV. One readily sees that the values for EA_{ad}, EA_{vert}, and VDE are different due to the difference in geometries between the neutral $AlAs_3$ (distorted rhombus) and the anion $AlAs_3^-$ (distorted tetrahedron).

Al_3As and Al_3As^-

The cyclic planar C_{2v} symmetry structure of the $^1A_1$ ground state for the neutral Al_3As and the same structure of the $^2B_2$ ground state for the anionic Al_3As^- are shown in 6n and 6a in Figure 1. The Al-As and As-As bond distances and Al-As-Al bond angle obtained by Archibong and St-Amant [8] at the CCSD(T) level were reported as 2.616, 2.389 Å and 111.4°, respectively. Our BP86 result of 2.605 Å (for the Al-As bond), 2.383 Å (for the As-As bond) and 111.0° (for the Al-As-Al bond angle) agree very well with their results. Our other three DFT functionals predict longer Al-As bonds with the longest being the value 2.646 Å given by BHLYP.

The C_{2v} symmetry of the $^2B_2$ ground state Al_3As^- is given in 6a in Figure 1. The Al1-As3 bond lengths given by the four DFT methods are longer than those for the Al2-As3 bonds, by 0.2 Å, and the two Al-As bonds are shorter than the Al-Al bonds by the four DFT methods. Archibong et al. [8] reported the Al1-Al2, Al1-As3 and Al2-As3 bond distances as 2.690, 2.644 and 2.450 Å at the MP2/6-311+G(2df) level. Our B3LYP method predicts the 2.695, 2.645 and 2.447 Å for the Al1-Al2, Al1-As3 and Al2-As3 bonds, giving the most reliable bond lengths for comparison with the MP2.

The EA_{ad}, EA_{vert}, and VDE values are reported in Table 4. Our predicted EA_{ad} is in the range from 1.52 to 1.88 eV, among which the BHLYP method predicts the largest value, EA_{ad} = 1.88 eV, which is different from the above clusters. The range of EA_{vert} is predicted from 1.20 to 1.57 eV. The range of VDE is from 1.77 to 2.09 eV. Again, the BP86 method yields the highest VDE value. But this is not the case for EA_{ad} and EA_{vert}. Archibong et al. [8] also gave their calculated EA_{ad} and VDE values of 1.80 eV and 2.02 eV at the CCSD(T) level, agreeing very well with our B3LYP results.

3.4 m + n = 5

Al_2As_3 and $Al_2As_3^-$

Both Al_2As_3 and $Al_2As_3^-$ have D_{3h} trigonal bipyramidal structures, which are given in 7n and 7a in Figure 1. For the neutral $^2A_2''$ ground state, the Al-As bond lengths given by the four DFT methods are all longer than those for the As-As bonds, by ~0.02 Å. Feng and Balasubramanian [9] studied the Al_2As_3 structure. They reported the Al-As and As-As distance to be 2.560 and 2.556 Å, respectively, using the CASSCF/MRSDCI level of theory with the RECPs basis sets. Our B3LYP bond distance 2.564 and 2.546 Å are all close to the Feng [9] prediction.

For the $^1A_1'$ ground state of $Al_2As_3^-$, the symmetry does not change, but the As-As bond lengths are shorter than those of the neutral species by ~0.06 Å, and the Al-As bond lengths are longer by ~0.1 Å. Feng and Balasubramanian [9] also optimized the anionic $Al_2As_3^-$ structure, predicting the bond distances to be 2.658 Å (Al-As) and 2.495 Å (As-As) at the CASSCF/ MRSDCI level. Their bond lengths are in good agreement with our B3LYP bond distances.

The theoretical EA_{ad}, EA_{vert}, and VDE are listed in Table 4. The range of EA_{ad} is from 2.11 to 2.32 eV. Again, the BP86 method predicted the largest EA_{ad} for Al_2As_3 (2.32 eV). The range of EA_{vert} is from 1.88 to 2.11 eV and the range of VDE is from 2.34 to 2.55 eV. The values for EA_{ad}, EA_{vert}, and VDE are fairly similar due to the small differences in geometry between neutral and anion, as for $AlAs_2$, Al_2As and Al_3As discussed above.

Al_3As_2 and $Al_3As_2^-$

The C_s symmetry structure of the $^2A'$ ground state for the neutral Al_3As_2 and the D_{3h}-symmetry structure of the $^1A_1'$ ground state for the anionic $Al_3As_2^-$ are shown in 8n and 8a in Figure 1. Feng and Balasubramanian [9] reported a distorted trigonal bipyramid structure with $C_{2v}(^2A_1)$ symmetry as the ground state. Our optimized BHLYP result is in agreement with their conclusion, but the other three DFT methods predict this C_{2v} structure a transition state with imaginary frequencies at 30, 100, and 104 cm^{-1}, respectively. Further optimization results in a geometry with lower C_s symmetry, which is more stable than the C_{2v} one by 0.10, 0.11, 0.09, and 0.16 eV at the BHLYP, B3LYP, BP86, and BLYP levels, respectively.

The $Al_3As_2^-$ ion displays D_{3h} symmetry, which is in agreement with the prediction of Feng et al. [9]. The BLYP method predicts the longest Al-As (2.599 Å) and As-As (2.629 Å) bond distances which compares well with Feng's values of 2.574 and 2.616 Å, respectively, obtained using CASSCF/MRSDCI level of theory with the RECPs basis set.

The theoretical EA_{ad}, EA_{vert}, and VDE are listed in Table 4. The range of EA_{ad} is from 2.60 to 2.98 eV from the four different functionals. The BHLYP result (2.98 eV) is the largest. The EA_{vert} values are ranging from 2.27 to 2.58 eV, and the VDE values are large and vary from 2.72 to 2.99 eV with BP86 giving the largest value (2.99 eV). One readily sees that the values for EA_{ad}, EA_{vert}, and VDE are different due to the large difference in structure between the neutral and anion.

$AlAs_4$ and $AlAs_4^-$

The C_{2v}-symmetry geometry of the $^2A_1$ ground state for $AlAs_4$ and the square pyramidal structure of C_{4v}-symmetry for the $^1A_1$ ground state for $AlAs_4^-$ are given in 9n and 9a in Figure 1. The neutral $AlAs_4$ can be seen as a tetrahedral As_4 structure with a two-fold Al atom bond to it, which is similar with the valence-isoelectronic $GaAs_4$ reported by Piquini et al. [30]. There exists two kinds of As-As and one Al-As bond in the neutral ground state, and the Al-As bond lengths given by the four DFT methods are all longer than those for As3-As5 bonds by about 0.1 Å and shorter than those for As2-As3 bonds by about 0.02 Å. The BLYP method, deemed to be the most reliable, gives bond lengths of 2.523 Å (for Al-As), 2.543 Å (for As2-As3) and 2.453 Å (for As3-As5). The other methods predict bond distances shorter by up to 0.1 Å. We also tried to optimize structures for the C_{4v}, C_s, and other C_{2v} symmetry of $AlAs_4$, but these stationary points all have higher energies and some have one imaginary vibrational frequency.

With attachment of an extra electron to the neutral $AlAs_4$ to form the $AlAs_4^-$ anion, the symmetry changes from C_{2v} to C_{4v}, the Al-As bond distances are longer than those of the neutral species by about 0.3 Å. And the four same Al-As bond distances are longer than the four equivalent As-As bonds by about 0.4 Å in the four DFT methods.

The theoretical EA_{ad}, EA_{vert}, and VDE are listed in Table 4. The predicted EA_{ad} for $AlAs_4$ ranges from 2.16 to 2.40 eV, among which the BP86 method again gives the highest EA_{ad} (2.40 eV). The EA_{vert} ranges from 1.28 to 1.45 eV. The VDE ranges from 3.06 to 3.26 eV, indicating that the anion is quit stable with respect to electron detachment. Again, the differences between EA_{ad}, EA_{vert}, and VDE are due to the changes in geometry between $AlAs_4$ and $AlAs_4^-$.

Al_4As and Al_4As^-

The C_{2v} symmetry structure of the $^2A_1$ ground state for the neutral Al_4As and the C_{2v}-symmetry structure of the $^1A_1$ ground state for the anionic Al_4As^- are shown in 10n and 10a in Figure 1. No other theoretical data available. For the neutral Al_4As, the As1-Al2 bond lengths given by the four DFT methods are shorter than those for the As1-Al3 bonds, by –0.06 Å, which are all shorter than the Al2-Al3 and Al2-Al5 bonds. The BLYP method gives the longest bond lengths of 2.430 Å (for As1-Al2), 2.487 Å (for As1-Al3), 2.830 Å (for Al2-Al3) and 2.646 Å (for Al3-Al5). The other methods predict bond distances shorter by up to 0.1 Å. The BLYP bond distances are considered to be the most reliable results based on the calculations above.

With attachment of an extra electron to the neutral Al_4As to form the Al_4As^- anion, the geometry does not change. The Al_4As^- anion still displays C_{2v} symmetry.

The theoretical EA_{ad}, EA_{vert}, and VDE are listed in Table 4. The BP86 method gives the highest values of EA_{ad} (1.94 eV), EA_{vert} (1.90 eV), and VDE (2.07 eV). Our other three functionals predict lower results with the lowest being the value 1.65, 1.61 and 1.68 eV given by BLYP. Again, the values for EA_{ad}, EA_{vert}, and VDE are different due to the differences in geometry between Al_4As and Al_4As^-.

4 Vibrational frequencies

Harmonic vibrational frequencies have been predicted for each neutral molecule with each functional, and these are reported in Table 5. Available theoretical prediction [8,10] is included for comparison. The B3LYP method gives the best predictions for the harmonic vibrational frequencies of the Al_mAs_n series, compared to the limited other theoretical results in Table 5. For the Al_mAs_n molecules, the average error for the B3LYP method is only about 10 cm^{-1}. The other three methods underestimate or overestimate the harmonic vibrational frequencies in the Al_mAs_n series, with the worst predictions given by the BHLYP method. Note that this emphasizes the necessity of being very selective in choosing DFT results for the theory predictions. The harmonic vibrational frequencies for the anionic $Al_mAs_n^-$ systems are listed in Table 6, which were also reported by Archibong et al. [8] and Zhu [10]. Our B3LYP vibrational frequencies for $Al_mAs_n^-$ are also in good agreement with their results.

Table 5. Harmonic vibrational frequencies (cm^{-1}) for Al_mAs_n ($m+n=2$–5).

	Sym.	BHLYP	B3LYP	BP86	BLYP	other theory
AlAs	σ	368	366	370	355	282 [7]
$AlAs_2$	b_2	105	100	101	90	97 [10]
	a_1	255	242	242	228	241 [10]
	a_1	413	385	373	360	385 [10]
Al_2As	a_1	39	57	40	55	58 [10]
	b_2	211	114	201	198	75 [10]
	a_1	352	345	349	332	343 [10]
$AlAs_3$	b_1	133	126	122	120	124 [8] 126 [8]
	a_1	221	206	201	192	202 [8] 206 [8]
	a_1	230	217	213	205	223 [8] 217 [8]
	b_2	230	229	237	220	269 [8] 229 [8]
	a_1	366	347	344	327	362 [8] 347 [8]
	b_2	429	401	391	376	412 [8] 401 [8]
Al_3As	b_1	93	99	102	101	120 [8] 99 [8]
	a_1	119	130	136	132	157 [8] 130 [8]
	a_1	223	235	249	234	277 [8] 234 [8]
	b_2	269	281	301	276	347 [8] 280 [8]
	b_2	353	337	331	320	362 [8] 337 [8]
	a_1	356	344	341	328	358 [8] 344 [8]
Al_2As_2	b_{3u}	75	72	70	70	
	b_{2u}	133	129	133	123	
	b_{3g}	184	181	190	173	
	a_g	265	255	255	243	
	b_{1u}	281	268	266	253	
	a_g	358	338	332	318	
Al_2As_3	e'	156	150	152	144	
	e''	211	205	213	195	
	a''_2	230	258	276	258	
	e'	248	234	234	222	
	a'_1	279	265	263	251	
	a'_1	366	349	348	331	
Al_3As_2	a''	38	47	34	57	
	a'	43	53	50	64	
	a'	109	129	144	139	
	a'	127	136	172	146	
	a''	140	177	212	184	
	a'	231	230	231	221	
	a''	266	247	253	230	
	a'	279	283	285	270	
	a'	322	312	315	300	
$AlAs_4$	b_1	46	47	38	50	
	a_1	159	147	139	137	
	a_2	197	180	175	164	
	a_1	216	201	199	189	
	b_1	218	203	200	191	
	b_2	261	241	235	223	
	a_1	312	289	286	269	
	a_1	336	314	310	294	
	b_2	340	317	315	294	
Al_4As	b_1	27	24	14	22	
	a_2	74	71	61	65	
	a_1	100	104	116	101	
	b_2	123	135	148	131	
	b_2	172	165	184	159	
	a_1	242	236	238	227	
	a_1	274	269	280	259	
	b_2	303	291	288	277	
	a_1	326	318	326	304	

Table 6. Harmonic vibrational frequencies (cm^{-1}) for anionic $Al_mAs_n^-$ ($m+n=2$–5).

	Sym.	BHLYP	B3LYP	BP86	BLYP	other theory
$AlAs^-$	σ	391	425	423	408	
$AlAs_2^-$	b_2	213	203	205	191	200 [10]
	a_1	308	288	283	270	286 [10]
	a_1	371	348	341	327	344 [10]
Al_2As^-	a_1	70	72	60	56	58 [10]
	a_1	372	352	344	331	345 [10]
	b_2	392	379	372	363	378 [10]
$AlAs_3^-$	a'	106	107	122	106	124 [8] 107 [8]
	a''	155	157	171	155	71 [8] 156 [8]
	a'	206	196	196	185	196 [8] 196 [8]
	a''	247	237	239	224	256 [8] 237 [8]
	a'	303	280	269	259	296 [8] 279 [8]
	a'	338	321	319	302	341 [8] 332 [8]
Al_3As^-	b_1	68	69	67	67	95 [8] 69 [8]
	a_1	135	142	159	142	132 [8] 142 [8]
	a_1	214	204	206	195	224 [8] 204 [8]
	b_2	240	248	264	242	262 [8] 248 [8]
	b_2	329	315	314	301	325 [8] 315 [8]
	a_1	329	316	316	301	327 [8] 316 [8]
$Al_2As_2^-$	a_1	51	56	63	57	
	b_1	152	152	157	146	
	a_2	173	166	173	154	
	a_1	260	244	242	230	
	a_1	329	312	308	292	
	b_2	329	314	312	296	
$Al_3As_2^-$	e'	97	97	98	96	
	e''	154	155	170	150	
	a''_2	193	187	191	178	
	a'_1	227	216	213	206	
	e'	313	300	99	283	
	a'_1	316	303	302	288	
$Al_2As_3^-$	e'	129	124	128	118	
	e''	156	153	164	145	
	e'	245	232	232	219	
	a'_1	283	269	269	255	
	a''_2	308	291	289	273	
	a'_1	331	313	313	296	
$AlAs_4^-$	b_2	104	98	97	93	
	e	122	121	132	116	
	b_2	184	167	157	154	
	a_1	268	255	255	240	
	e	284	263	258	243	
	a_1	311	289	285	269	
	b_1	313	291	285	270	
Al_4As^-	b_1	28	23	14	21	
	a_2	74	62	37	50	
	a_1	97	92	97	86	
	b_2	162	161	172	153	
	b_2	237	225	225	211	
	a_1	244	231	228	217	
	a_1	300	288	292	272	
	b_2	319	304	302	287	
	a_1	257	333	327	311	

5 Conclusions

Carefully selected DFT methods applied with the 6-311+G(2df) basis set are capable of reliably predicting the available experimental structures, EAs, and vibrational frequencies for the neutral and anionic aluminum arsenides clusters. The best method for predicting molecular structures was found to be BLYP, while other methods generally underestimated bond lengths. The largest adiabatic electron affinities, vertical electron affinity and vertical detachment energy, obtained at the 6-311+G(2df)/BP86 level of theory, are 2.20, 2.04 and 2.27 eV (AlAs), 2.13, 1.94 and 2.38 eV ($AlAs_2$), 2.44, 2.39 and 2.47 eV (Al_2As), 2.09, 1.80 and 2.53 eV (Al_2As_2), 2.01, 1.57 and 2.36 eV ($AlAs_3$), 2.32, 2.11 and 2.55 eV (Al_2As_3), 2.40, 1.45 and 3.26 eV ($AlAs_4$),1.94, 1.90 and 2.07 eV (Al_4As), respectively. However, the BHLYP method is largest for the EA_{ad} and EA_{vert} of Al_3As. For the vibrational frequencies of the $\mathrm{Al}_m\mathrm{As}_n$ series, the B3LYP method produces good predictions with the average error only about 10 cm^{-1} from available experimental and theoretical values. The other three methods overestimate or underestimate the vibrational frequencies, with the worst predictions given by the BHLYP method.

This work was financially supported by the National Natural Science Foundation of China (Grant No. 20603021) and the Youth Academic Leader of Shanxi.

References

1. H. Gomez, T.R. Taylor, D.M. Neumark, J. Phys. Chem. A **105**, 6886 (2001)
2. K. Balasubramanian, P.Y. Feng, J. Phys. Chem. A **105**, 11295 (2001)
3. T.R. Taylor, H. Gomez, K.R. Asmis, D.M. Neumark, J. Chem. Phys. **115**, 4620 (2001)
4. W. Andreoni, Phys. Rev. B. **45**, 4203 (1992)
5. H.K. Quek, Y.P. Feng, C.K. Ong, Z. Phys. D **42**, 309 (1997)
6. V. Tozzini, F. Buda, A. Fasolino, J. Phys. Chem. B **105**, 12477 (2001)
7. A. Costales, A.K. Kandalam, R. Franco, R. Pandey, J. Phys. Chem. B **106**, 1940 (2002)
8. E.F. Archibong, A. St-Amant, J. Phys. Chem. A **106**, 7390 (2002)
9. P.Y. Feng, D. Dai, K. Balasubramanian, J. Phys. Chem. A **104**, 422 (2000)
10. X. Zhu, J. Mol. Struct. (Theochem) **638**, 99 (2003)
11. P. Hohenberg, W. Kohn, Phys. Rev. B **136**, 864 (1964); W. Kohn, L. Sham, Phys. Rev. A **140**, 1133 (1965)
12. W. Kohn, A.D. Becke, R.G. Parr, J. Phys. Chem. **100**, 12974 (1996)
13. E.F. Achibong, A. St-Amant, Chem. Phys. Lett. **316**, 151 (2000)
14. S.K. Nayak, S.N. Khanna, P. Jena, Phys. Rev. B **57**, 3787 (1998)
15. A. Costales, R. Pandey, J. Phys. Chem. A **107**, 192 (2003)
16. C. Lee, W. Yang, R.G. Parr, Phys. Rev. B **37**, 785 (1993)
17. A.D. Becke, J. Chem. Phys. **98**, 1372 (1993)
18. A.D. Becke, J. Chem. Phys. **98**, 5648 (1993); P.J. Stephens, F.J. Devlin, C.F. Chabalowski, M.J. Frisch, J. Phys. Chem. **98**, 11623 (1994)
19. J.P. Perdew, Phys. Rev. B **34**, 7406 (1986)
20. M.J. Frisch, G.W. Trucks, H.B. Schlegel, G.E. Scuseria, M.A. Robb, J.R. Cheeseman, V.G. Zakrzewski, J.A. Montgomery Jr, R.E. Stratmann, J.C. Burant, S. Dapprich, J.M. Millam, A.D. Daniels, K.N. Kudin, M.C. Strain, O. Farkas, J. Tomasi, V. Barone, M. Cossi, R. Cammi, B. Mennucci, C. Pomelli, C. Adamo, S. Clifford, J. Ochterski, G.A. Petersson, P.Y. Ayala, Q. Cui, K. Morokuma, D.K. Malick, A.D. Rabuck, K. Raghava-chari, J.B. Foresman, J. Cioslowski, J.V. Ortiz, B.B. Stefanov, G. Liu, A. Liashenko, P. Piskorz, I. Komaromi, R. Gomperts, R.L. Martin, D.J. Fox, T. Keith, M.A. Al-Laham, C.Y. Peng, A.Nanayakkara, C. Gonzalez, M. Challacombe, P.M.W. Gill, B.Johnson, W. Chen, M.W. Wong, J.L. Andres, C. Gonzalez, M. Head-Gordon, E.S. Replogle, J.A. Pople, computer code Gaussian98, revision A.6 (Gaussian, Inc., Pittsburgh, PA, 1998)
21. E.F. Archibong, A. St-Amant, J. Chem. Phys. **109**, 962 (1998)
22. E.F. Achibong, A. St-Amant, Chem. Phys. Lett. **284**, 331 (1998)
23. E.F. Achibong, A. St-Amant, J. Phys. Chem. A **102**, 6877 (1998)
24. E.F. Achibong, A. St-Amant, J. Phys. Chem. A **103**, 1109 (1999)
25. E.F. Achibong, A. St-Amant, Chem. Phys. Lett. **316**, 151 (2000)
26. A.D. McLean, G.S. Chandler, J. Chem. Phys. **72**, 5639 (1980)
27. M.J. Frisch et al. (Gaussian 94, Gaussian, Pittsburgh, PA, 1995)
28. Z.Y. Liu, C.R. Wang, R.B. Huang, Int. J. Mass Spectrom. Ion Proc. **4**, 201 (1995)
29. E.F. Achibong, A. St-Amant, J. Phys. Chem. A **106**, 7390 (2002)
30. P. Piquini, S. Canuto, A. Fazzio, Nanostruct. Mat. **10**, 635 (1998)
31. M.D. Chen, R.B. Huang, Chem. Phys. Lett. **325**, 22 (2000)
32. R.O. Jones, D. Hohl, J. Chem. Phys. **92**, 6710 (1990)
33. T.R. Talor, K.R. Asmis, C. Xu, D.M. Neumark, Chem. Phys. Lett. **297**, 133 (1998)